Catal Lett
DOI 10.1007/s10562-017-2051-3

Highly Efficient and Convenient Supported Ionic Liquid $TiCl_5$-DMIL@SiO_2@Fe_3O_4-Catalyzed Cycloaddition of CO_2 and Epoxides to Cyclic Carbonates

Yu Lin Hu[1,2] · **Rong Xing**[3]

Received: 24 January 2017 / Accepted: 2 April 2017

Abstract A series of silica coated magnetic nanoparticles supported ILs were prepared, characterized and their catalytic performances in cycloaddition of CO_2 to epoxides were investigated. The influences of various reaction parameters including catalyst selection, catalyst amount, reaction time, and reaction temperature were studied. Research shows that $TiCl_5$-DMIL@SiO_2@Fe_3O_4 could be used as the highest efficient catalyst in cycloaddition of CO_2 and epoxides to gives the corresponding cyclic carbonates. Good to excellent yields were achieved for this reaction under mild conditions. The heterogeneous supported catalyst is easily recoverable by filtration, and could be used for five consecutive runs without significant loss in catalytic activity.

Graphical Abstract

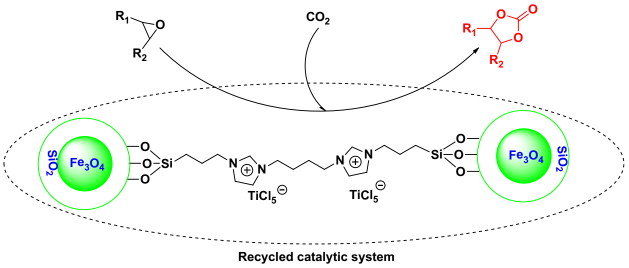

Keywords Supported ionic liquid · Cycloaddition · Epoxides · CO_2 · Heterogeneous catalysis

1 Introduction

Carbon dioxide is an attractive C1 source that have been widely used for the production of a variety of chemicals [1, 2]. Nowadays, numerous methods have been developed for the preparation of these molecules, and one of the most attractive synthetic protocols constitutes the cycloaddition of CO_2 to epoxides to afford cyclic carbonates [3]. Conventionally, the common protocol for the assembly of these compounds is the use of alkali metal catalysts [4, 5]. However, these protocols suffered from some drawbacks such as the use of stoichiometric amount of catalysts and generation of vast amounts of corrosive wastes. In order to overcome these problems, many efforts have been developed for this transformation, and various catalysts have been developed including PS-TBMAC/ZnI_2 [6], salen-complexes [7–11], bromide [12], $K_2S_2O_8$/NaBr [13], MOFs [14–21], quaternary ammonium hydroxide [22], supported imidazole [23], organocatalysts [24, 25], and others [26–29]. However, some of these procedures still require

---

✉ Yu Lin Hu
huyulin1982@163.com

[1] College of Materials and Chemical Engineering, China Three Gorges University, Yichang 443002, People's Republic of China

[2] Key Laboratory of Inorganic Nonmetallic Crystalline and Energy Conversion Materials, China Three Gorges University, Yichang 443002, People's Republic of China

[3] College of Chemistry and Environmental Engineering, Yancheng Teachers University, Yancheng 224002, People's Republic of China

harsh reaction condition, the cost and instability of catalysts. Therefore, the design and explore of environmentally benign and efficient catalysts that address these drawbacks are highly desirable.

Ionic liquids (ILs) are well-known green reaction media and catalysts because of their outstanding and unique properties [30–32]. Examples of their applications in the synthesis of cyclic carbonates from CO_2 and epoxides were reported [33–37]. Although their good catalytic activities in the reaction, they have some problems such as partially ILs wasted and difficulties in separating catalysts from products after the reaction. Immobilized ILs have the attractive features of ILs and heterogeneous catalysis, such as easy catalyst recovery, high efficiency, high stability and recyclability. Thus, this problem can be overcome by immobilizing the traditional IL on solid supports [38–46]. Various methods have been developed for immobilization of ILs on solid supports such as alumina, titania, silica, etc, and among these solid supports, silica was found to be one of the most effective one [41]. In the present study, a series of silica coated magnetic nanoparticles supported functionalized ionic liquids anion-DMIL@SiO_2@Fe_3O_4 have been prepared and characterized, which exhibited good chemical and thermal stability, and were applied as a novel heterogeneous catalyst in the preparation of cyclic carbonates by cycloaddition of CO_2 to epoxides (Scheme 1). As well as this, the reusability of the supported functionalized IL was also studied.

2 Experimental

2.1 General

The reagents and solvents were purchased from Aldrich. All the chemicals were from commercial sources without any pretreatment. Powder X-ray diffraction (XRD) patterns were collected on a Rigaku Ultima IV diffractometer. Scanning electron microscopy (SEM) and Energy dispersive X-ray (EDX) analysis were carried out on a JSM-7500F Scanning Electron Microscope. FTIR spectra were recorded on a Nicolet Nexus 470 Fourier transform infrared spectrometer. UV–Vis spectra were recorded on a Shimadzu UV-2450 spectrometer. Magnetic properties were carried out using a vibrating sample magnetometer (PPMS-9T, Quantum Design, USA) in the magnetic field range of −10,000 to 10,000 Oe at room temperature. Thermogravimetric analysis (TG) were measured on a Netzsch Thermoanalyzer STA 449. GC experiments were performed on a Shimadzu GC-2014C chromatograph. ^1H NMR spectra were recorded in $CDCl_3$ at room temperature on a Bruker 400 MHz spectrometer. Elemental analysis were performed on a Vario EL III instrument.

2.2 Supported ILs Anion-DMIL@SiO_2@Fe_3O_4 Preparation

Supported ILs were prepared according to reported process [40–44] and shown in Scheme 2. Preparation of SiO_2@Fe_3O_4: Fe_3O_4 (2 g), ethanol (400 mL) were sonicated at room temperature for 60 min, and tetraethyl orthosilicate (4 mL), $NH_3{\cdot}H_2O$ (28%) (12 mL) were added. The mixture was stirred at room temperature for 24 h. The nanoparticles were isolated by filtration and washed with H_2O (3 × 20 mL), EtOH (3 × 20 mL), and dried under vacuum to afford the silica-coated Fe_3O_4 nanoparticles. Preparation of Cl-DMIL: 1,4-di(1H-imidazol-1-yl)butane (0.5 mol), (3-chloropropyl) triethoxysilane (2.2 mol), toluene (400 mL) were refluxed for 36 h under N2 atmosphere, and then the solvent was removed by liquid–liquid separation, and the residue was evaporated under vacuum to give Cl-DMIL. Preparation of anion-DMIL: Cl-DMIL (0.05 mol) was dispersed in CH_2Cl_2/CH_3CN (120 mL) and stirred vigorously with KPF_6 (0.11 mol)/$ZnCl_2$ or $TiCl_4$ (0.11 mol) for 24 h under reflux conditions. After cooled down to room temperature, the resulting material was isolated by filtration, washed with H_2O (3 × 20 mL), EtOH (3 × 20 mL), and evaporated under vacuum to give PF_6-DMIL, $ZnCl_3$-DMIL

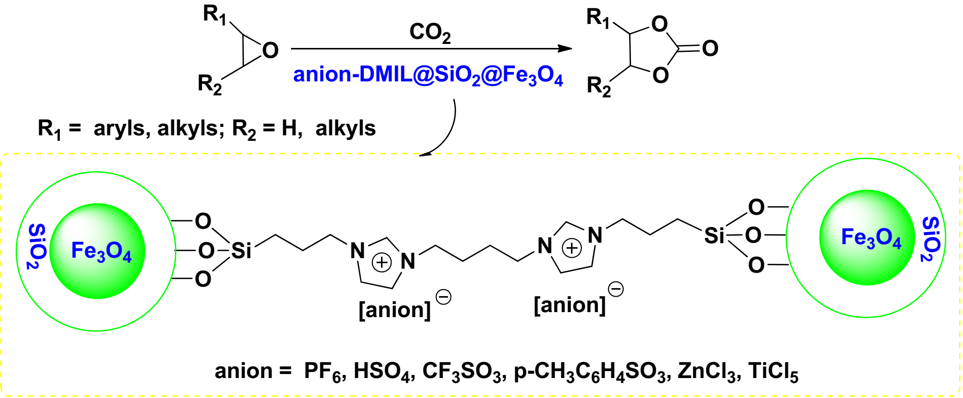

Scheme 1 Catalytic preparation of cyclic carbonates by cycloaddition of CO_2 to epoxides

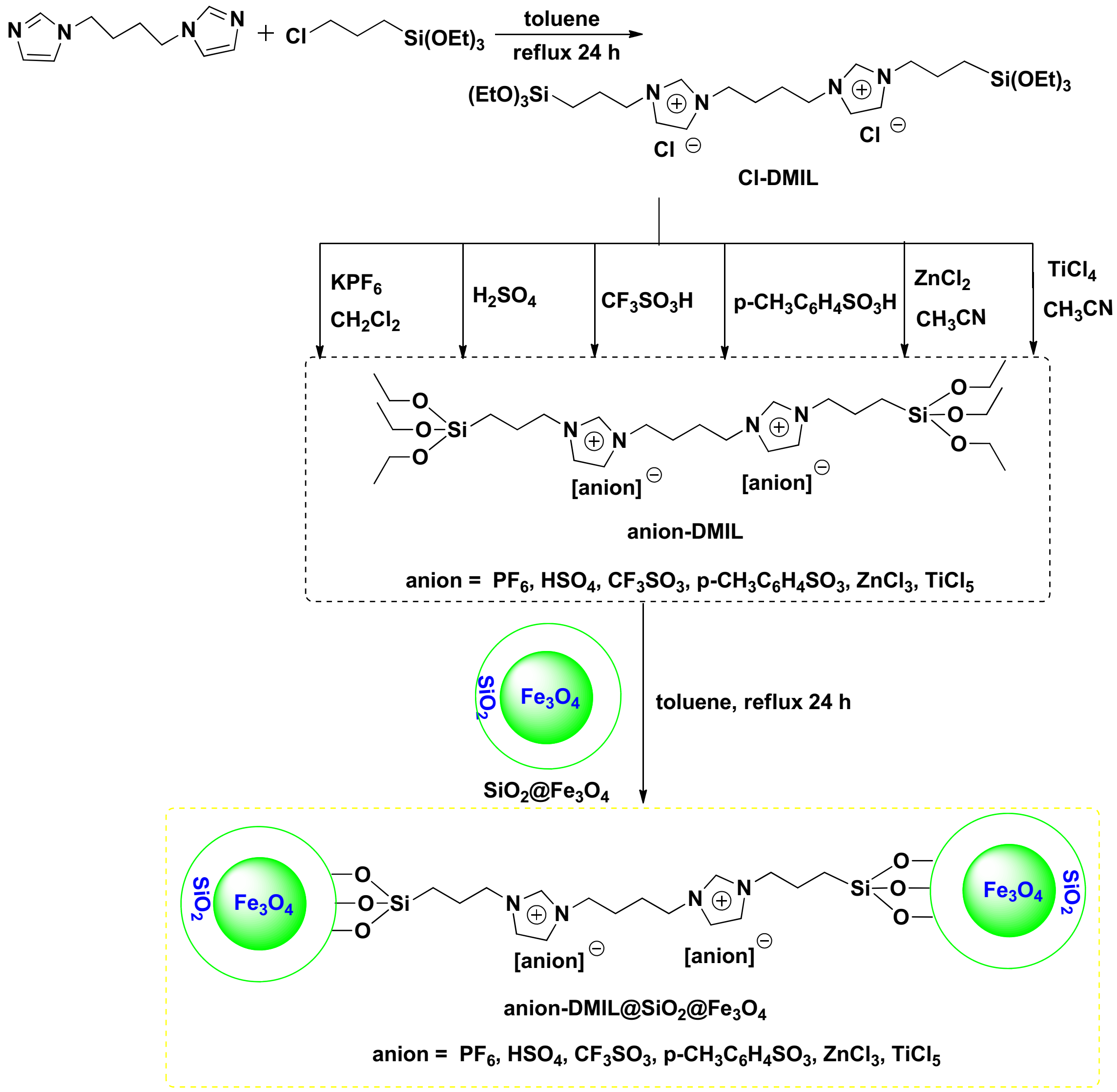

Scheme 2 Preparation of supported ILs

or $TiCl_5$-DMIL; Cl-DMIL (0.05 mol), H_2SO_4, p-$CH_3C_6H_4SO_3H$ or CF_3SO_3H (0.1 mol) were stirred vigorously at 50 °C for 12 h, then the resulting material was dried under vacuum to give HSO_4-DMIL, p-$CH_3C_6H_4SO_3$-DMIL or CF_3SO_3-DMIL. Preparation of anion-DMIL@SiO_2@Fe_3O_4: anion-DMIL (0.01 mol), SiO_2@Fe_3O_4 (3 g), and toluene (400 mL) were stirred under reflux conditions for 24 h. The resultant solid was separated magnetically and washed with EtOH (3 × 20 mL) and dried under vacuum.

2.3 General Procedure for Catalytic Cycloaddition of Epoxides with CO_2

Typically, epoxide (0.1 mol) and $TiCl_5$-DMIL@SiO_2@Fe_3O_4 (0.5 g) were introduced into a stainless-steel autoclave. CO_2 was charged in the autoclave and the pressure was raised to 0.8 MPa at 100 °C. The reaction mixture was stirred at 100 °C for the desired time. The reaction progress was monitored by GC. When the pressure of reactor was fall down to a presetting value, then the excess of CO_2 was vented. The resulting mixture was distilled under vacuum to afford the desired pure product. Fresh substrates were then recharged to the recovered catalyst and then recycled under identical reaction conditions. All products were identified by comparing their physical and GC spectra with those of commercial materials.

2.4 Spectral Data of Products

2.4.1 4-Methyl-1,3-dioxolan-2-one (Table 2, Entry 1)

^{1}H NMR: δ 1.41 (dd, CH_3, 3H), 3.96 (m, CH, 1H), 4.52 (m, CH, 1H), 4.83 (m, CH, 1H). Anal. Calcd. for $C_4H_6O_3$:

C, 47.02; H, 5.89; O, 47.01. Found: C, 47.06; H, 5.92; O, 47.02.

2.4.2 *1,3-Dioxolan-2-one (Table 2, Entry 2)*

^{1}H NMR: δ 4.51 (s, CH_2CH_2, 4H). Anal. Calcd. for $C_3H_4O_3$: C, 40.89; H, 4.55; O, 54.47. Found: C, 40.92; H, 4.58; O, 54.50.

2.4.3 *4,4-Dimethyl-1,3-dioxolan-2-one (Table 2, Entry 3)*

^{1}H NMR: δ 1.43 (s, $2CH_3$, 6H), 4.21 (s, CH_2, 2H). Anal. Calcd. for $C_5H_8O_3$: C, 51.68; H, 6.91; O, 41.32. Found: C, 51.72; H, 6.94; O, 41.34.

2.4.4 *4-Propyl-1,3-dioxolan-2-one (Table 2, Entry 4)*

^{1}H NMR: δ 0.87 (t, CH_3, 3H), 1.38 (m, CH_2, 2H), 1.57 (dd, CH_2, 2H), 4.09 (m, CH, 1H), 4.53 (t, CH_2, 1H), 4.71 (t, CH_2, 1H). Anal. Calcd. for $C_6H_{10}O_3$: C, 55.32; H, 7.68; O, 36.81. Found: C, 55.34; H, 7.71; O, 36.85.

2.4.5 *4-(Chloromethyl)-1,3-dioxolan-2-one (Table 2, Entry 5)*

^{1}H NMR: δ 3.79 (dd, CH_2, 2H), 4.32 (dd, CH_2, 1H), 4.61 (dd, CH_2, 1H), 4.92 (m, CH_2, 1H). Anal. Calcd. for $C_4H_5ClO_3$: C, 35.13; H, 3.64; Cl, 25.91; O, 35.09. Found: C, 35.19; H, 3.69; Cl, 25.97; O, 35.15.

2.4.6 *Hexahydrobenzo[d] [1,3] dioxol-2-one (Table 2, Entry 6)*

^{1}H NMR: δ 1.83 (m, 2CH, 2H), 2.01 (m, 2CH, 2H), 2.31 (m, CH_2CH_2, 4H), 5.09 (m, 2CH, 2H). Anal. Calcd. for $C_7H_{10}O_3$: C, 59.11; H, 7.08; O, 33.75. Found: C, 59.14; H, 7.09; O, 33.77.

2.4.7 *4-Phenoxymethyl-1,3-dioxolan-2-one (Table 2, Entry 7)*

^{1}H NMR: δ 4.18 (m, CH_2, 2H), 4.61 (m, CH_2, 2H), 4.95 (m, CH, 1H), 6.91–7.06 (m, Ar–H, 3H), 7.35–7.42 (m, Ar–H, 2H). Anal. Calcd. for $C_{10}H_{10}O_4$: C, 61.81; H, 5.17; O, 32.93. Found: C, 61.85; H, 5.19; O, 32.96.

2.4.8 *4-Phenyl-1,3-dioxolan-2-one (Table 2, Entry 8)*

^{1}H NMR: δ 4.34 (t, CH_2, 1H), 4.77 (t, CH_2, 1H), 5.65 (t, CH_2, 1H), 7.31–7.48 (m, Ar–H, 5H). Anal. Calcd. for $C_9H_8O_3$: C, 65.85; H, 4.89; O, 29.21. Found: C, 65.85; H, 4.91; O, 29.24.

3 Results and Discussion

The characterization of the silica coated magnetic nanoparticles supported ILs were using FT-IR, SEM, EDX, and XRD analysis. The FT-IR spectra of the supported ILs are shown in Fig. 1. The characteristic bonds at about 1475, 1538, and 1660 cm^{-1}, which were assigned to the C–H bending vibrations, C=C and C=N stretching vibrations of the imidazolium ring [40]. The peaks observed at about 1090 and 980 cm^{-1} were belonged to the stretching vibration of Si–O–Si. The peaks at about 2975, 1320 cm^{-1} are attributed to C–H stretching of alkyl chain, and the peak at about 3480 cm^{-1} is related to C–H stretching of the absorbed water. The peaks observed at 1542, 1450 cm^{-1} (Fig. 1a), 1718, 875 cm^{-1} (Fig. 1b), 827 cm^{-1} (Fig. 1c), 1025 cm^{-1} (Fig. 1d), 575, 690, 822 cm^{-1} (Fig. 1e), and 1472, 1365, 1269 cm^{-1} (Fig. 1f), related to vibrational modes of $ZnCl_3$, HSO_4, PF_6, CF_3SO_3, p-$CH_3C_6H_4SO_3$, and $TiCl_5$ respectively. Moreover, the absorption band at about 575 cm^{-1} is attributed to the Fe–O stretching vibration of Fe_3O_4 [44].

The surface morphology and chemical composition of the supported ILs were analyzed by SEM and EDX. SEM images of the supported ILs are shown in Fig. 2, it clearly observed that all the ILs particles were well-defined, and the surface of the supported ILs are smooth and soft, which shows highly uniform particles. Figure 3 displayed the EDX analysis of the supported ILs. EDX obtained from SEM showed the presence of the expected elements in their structure. Figure 4 displayed the XRD diffractograms of the supported ILs. All of the supported

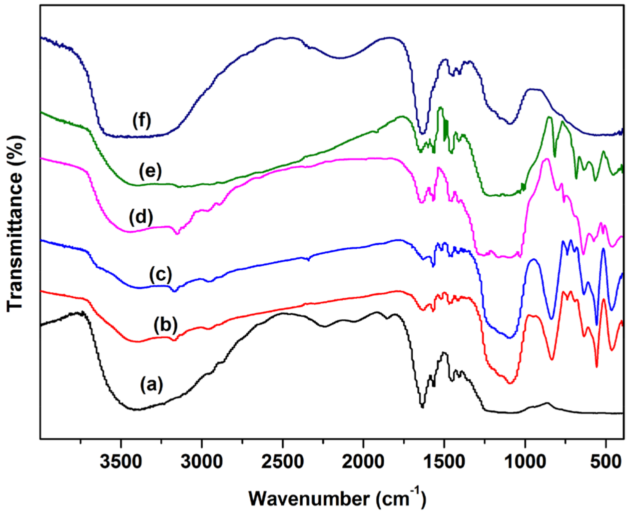

Fig. 1 FT-IR spectra of $ZnCl_3$-DMIL@SiO_2@Fe_3O_4 (*a*), HSO_4-DMIL@SiO_2@Fe_3O_4 (*b*), PF_6-DMIL@SiO_2@Fe_3O_4 (*c*), CF_3SO_3-DMIL@SiO_2@Fe_3O_4 (*d*), p-$CH_3C_6H_4SO_3$-DMIL @SiO_2@Fe_3O_4 (*e*), $TiCl_5$-DMIL@SiO_2@Fe_3O_4 (*f*)

ILs had the diffraction peaks of the cubic structure of Fe_3O_4 (JCPDS No.19-0629) [45]. The absence of obvious characteristic peaks of anions of ILs in the XRD patterns suggests that the anion is well-dispersed on the surface in the channels of the silica coated magnetic nanoparticles, and the broadness of the peaks shows the nanocrystalline nature of the prepared supported ILs. Figure 5 showed the diffuse reflectance UV–Vis spectra of the supported ILs. All the supported ILs exhibit a peak around 215 nm, which are assigned to the O–Si transition [38, 41]. In addition to this peak, another peaks appeared at around 413, 492, 556 nm in Fig. 5f, which is likely to

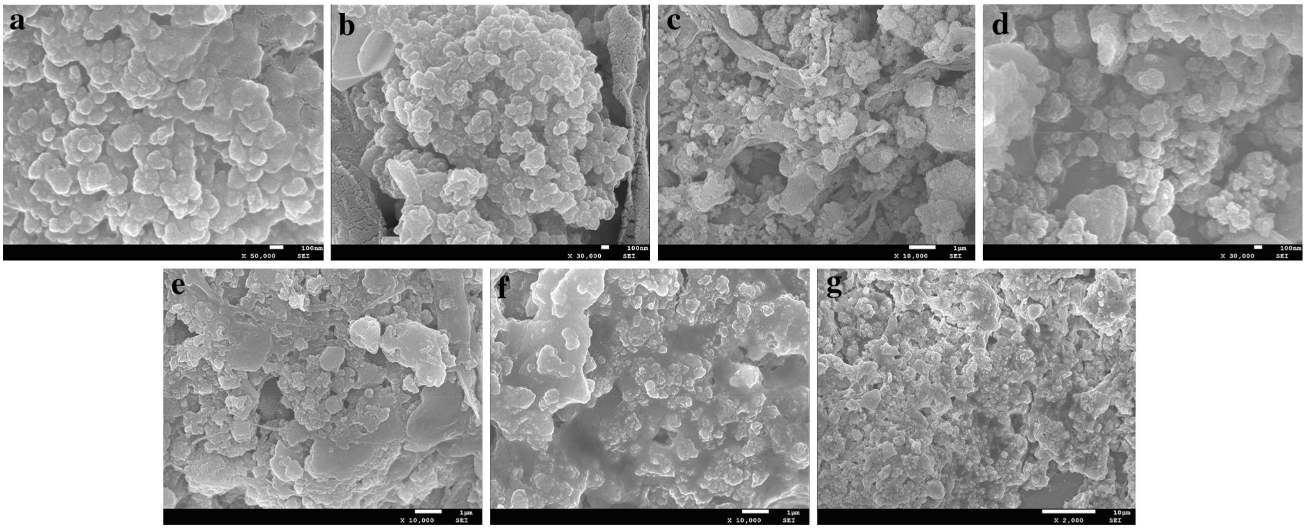

Fig. 2 SEM images of $ZnCl_3$-DMIL@SiO_2@Fe_3O_4 (**a**), HSO_4-DMIL@SiO_2@Fe_3O_4 (**b**), PF_6-DMIL@SiO_2@Fe_3O_4 (**c**), CF_3SO_3-DMIL@SiO_2@Fe_3O_4 (**d**), *p*-$CH_3C_6H_4SO_3$-DMIL@SiO_2@Fe_3O_4 (**e**), $TiCl_5$-DMIL@SiO_2@Fe_3O_4 (**f**), and five times recycled $TiCl_5$-DMIL@SiO_2@Fe_3O_4 (**g**)

Fig. 3 EDX images of $ZnCl_3$-DMIL@SiO_2@Fe_3O_4 (**a**), HSO_4-DMIL@SiO_2@Fe_3O_4 (**b**), PF_6-DMIL@SiO_2@Fe_3O_4 (**c**), CF_3SO_3-DMIL@SiO_2@Fe_3O_4 (**d**), *p*-$CH_3C_6H_4SO_3$-DMIL @SiO_2@Fe_3O_4 (**e**), $TiCl_5$-DMIL@SiO_2@Fe_3O_4 (**f**)

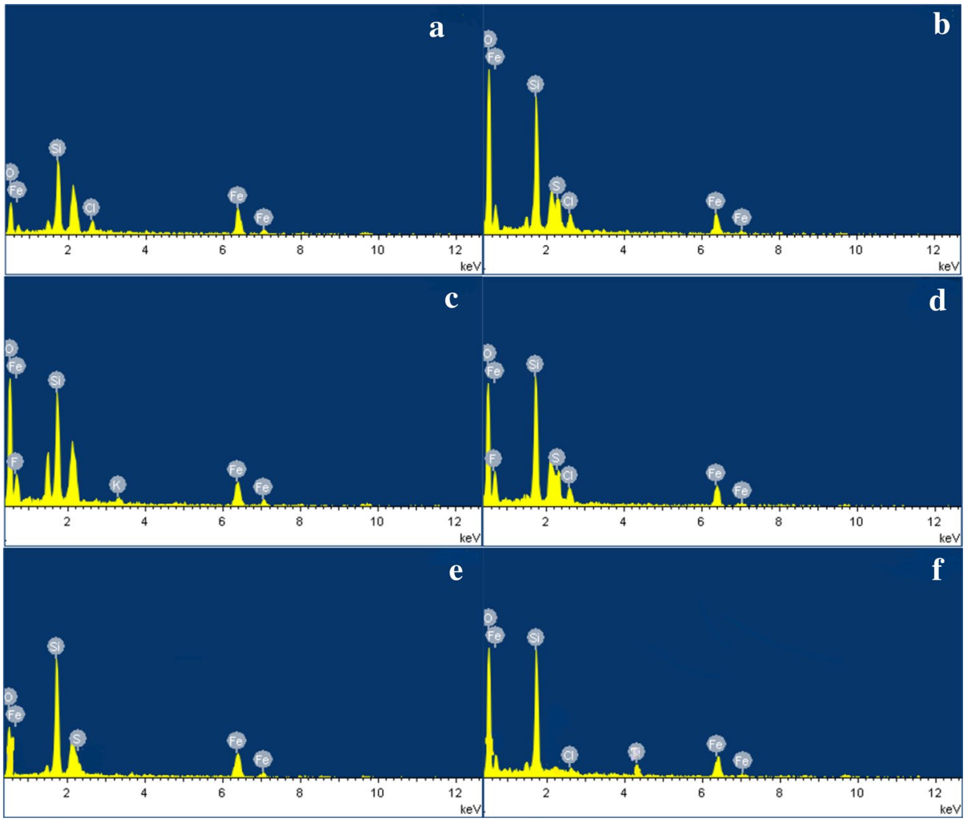

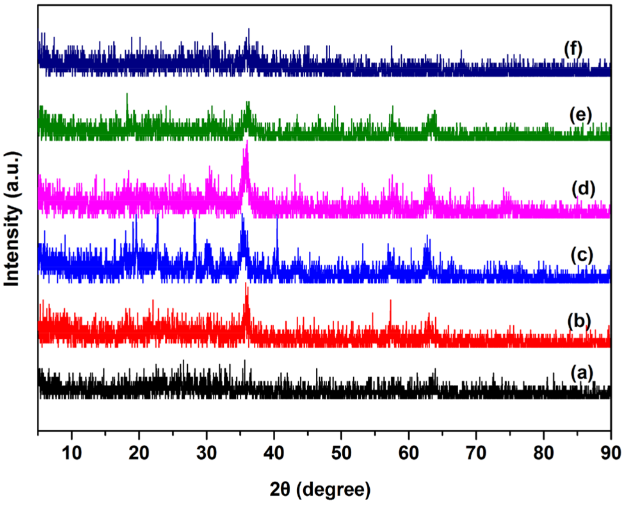

Fig. 4 XRD diffractograms of $ZnCl_3$-DMIL@SiO_2@Fe_3O_4 (*a*), HSO_4-DMIL@SiO_2@Fe_3O_4 (*b*), PF_6-DMIL@SiO_2@Fe_3O_4 (*c*), CF_3SO_3-DMIL@SiO_2@Fe_3O_4 (*d*), *p*-$CH_3C_6H_4SO_3$-DMIL @SiO_2@Fe_3O_4 (*e*), $TiCl_5$-DMIL@SiO_2@Fe_3O_4 (*f*)

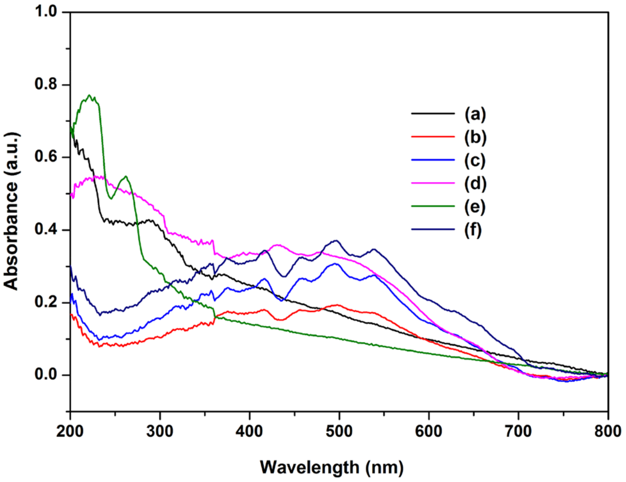

Fig. 5 UV–Vis spectra of $ZnCl_3$-DMIL@SiO_2@Fe_3O_4 (*a*), HSO_4-DMIL@SiO_2@Fe_3O_4 (*b*), PF_6-DMIL@SiO_2@Fe_3O_4 (*c*), CF_3SO_3-DMIL@SiO_2@Fe_3O_4 (*d*), *p*-$CH_3C_6H_4SO_3$-DMIL @SiO_2@Fe_3O_4 (*e*), $TiCl_5$-DMIL@SiO_2@Fe_3O_4 (*f*)

be associated with the characteristic absorption band of Ti–Cl [47–49].

In order to optimize the reaction conditions and test the catalytic activities of the synthesized supported ILs, initially we selected the cycloaddition of propylene oxide and CO_2 as a model reaction and the proper chosen of ILs were examined for this reaction. A series of supported IL catalysts such as $ZnCl_3$-DMIL@SiO_2@Fe_3O_4, HSO_4-DMIL@SiO_2@Fe_3O_4, PF_6-DMIL@SiO_2 @Fe_3O_4, CF_3SO_3-DMIL@SiO_2@Fe_3O_4, *p*-$CH_3C_6H_4SO_3$-DMIL @SiO_2@Fe_3O_4, and $TiCl_5$-DMIL@SiO_2@Fe_3O_4, were probed in the reaction (Table 1, entries 1–6). Among the supported ILs, $TiCl_5$-DMIL@SiO_2@Fe_3O_4 demonstrated the best results in terms of yield and reaction conditions (Table 1, entry 6). The contrast experiments were studied with bulk IL catalysts, such as $ZnCl_3$-DMIL, *p*-$CH_3C_6H_4SO_3$-DMIL, HSO_4-DMIL (Table 1, entries 7–9). Results show that the supported ILs showed much higher reaction efficiency than the bulk ILs, which might be due to the increase of the surface area of the catalyst after supported on silica coated magnetic nanoparticles carrier. Therefore, $TiCl_5$-DMIL@SiO_2@Fe_3O_4 was chosen as the suitable catalyst in the subsequent experiments.

It was found that the cycloaddition was significantly affected by the amount of supported catalyst (Fig. 6). The reaction did not perform in the absence of $TiCl_5$-DMIL@SiO_2@Fe_3O_4. As expected, the reaction activity was strengthened with the increase of the catalyst amount, the product yield and selectivity raised with the amount of catalyst increased to 0.5 g. However, there was no substantial change in the yield and selectivity with further increasing the amount of catalyst, while decreased the amount of catalyst resulted in lowering the yield and selectivity. Therefore, the best result was obtained by carrying out the reaction with a catalyst amount of 0.5 g.

The influence of CO_2 pressure on the cycloaddition were investigated (Fig. 7). It was found that the product yield and selectivity could be retained at a low CO_2 pressure, demonstrating the preferential effect of $TiCl_5$-DMIL@SiO_2@Fe_3O_4 for promoting the reactivity of CO_2. The reaction activity was strengthened as CO_2 pressure increased to 0.8 MPa, higher CO_2 pressure can effectively increase the solubility of CO_2 in propylene oxide, enabling the reaction equilibrium to shift towards cycloaddition. However, it was observed that a decrease in the yield and selectivity with the further increase of CO_2 pressure. The studies revealed that CO_2 pressure has important influence on the reaction, and 0.8 MPa was identified as the optimal CO_2 pressure.

Figure 8 showed the magnetization curves of the selected supported ILs such as PF_6-DMIL@SiO_2@Fe_3O_4, *p*-$CH_3C_6H_4SO_3$-DMIL@SiO_2@Fe_3O_4, and the catalyst $TiCl_5$-DMIL@SiO_2@Fe_3O_4, and the saturation magnetizations are 19.2, 21.7, and 49.8 emu/g, respectively. Compared to the magnetic property of SiO_2@Fe_3O_4 with saturation magnetization of about 60 emu/g [44], the $TiCl_5$-DMIL@SiO_2@Fe_3O_4 exhibited a superparamagnetic property with saturation magnetization of 49.8 emu/g, which is important for the supported catalyst in separation after the completion of the reaction.

The heterogeneous catalyst $TiCl_5$-DMIL@SiO_2@Fe_3O_4 can be easily separated and recovered by filtration after the reaction. The cycloaddition results by recovered $TiCl_5$-DMIL@SiO_2@Fe_3O_4 are shown in Fig. 9. The overall thermal stability of the supported IL was conducted

Table 1 Catalyst screening for the cycloaddition of propylene oxide and CO_2

Entry	Catalyst	Time (h)	Yield (%)[a]	Selectivity (%)[b]
1	$ZnCl_3$-DMIL@SiO_2@Fe_3O_4	2	91	97
2	HSO_4-DMIL@SiO_2@Fe_3O_4	3	64	83
3	PF_6-DMIL@SiO_2@Fe_3O_4	8	21	92
4	CF_3SO_3-DMIL@SiO_2@Fe_3O_4	3	72	78
5	*p*-$CH_3C_6H_4SO_3$-DMIL@SiO_2@Fe_3O_4	3	78	87
6	$TiCl_5$-DMIL@SiO_2@Fe_3O_4	2	95	99
7	$ZnCl_3$-DMIL	5	82	91
8	*p*-$CH_3C_6H_4SO_3$-DMIL	8	58	79
9	HSO_4-DMIL	8	46	75

Reaction conditions: propylene oxide (0.1 mol), catalyst (0.5 g), CO_2 (0.8 MPa), at 100 °C

[a] Isolated yield

[b] Isolated selectivity

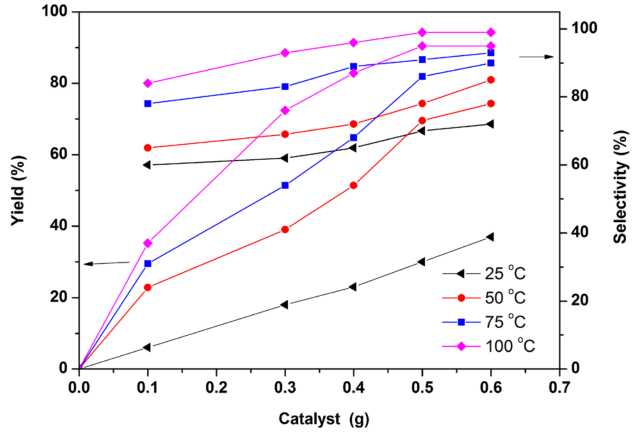

Fig. 6 Effect of the amount of catalyst on the cycloaddition. The reactions were carried out with propylene oxide (0.1 mol), CO_2 (0.8 MPa), in different amounts of $TiCl_5$-DMIL@SiO_2@Fe_3O_4 for 2 h

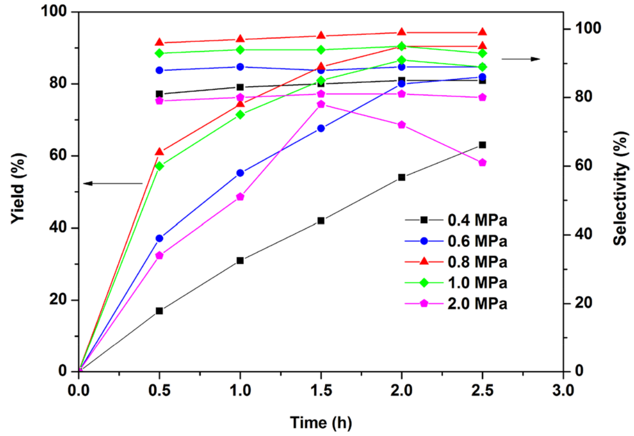

Fig. 7 Influence of CO_2 pressure on the cycloaddition. The reactions were carried out with propylene oxide (0.1 mol), $TiCl_5$-DMIL@SiO_2@Fe_3O_4 (0.5 g), in different CO_2 pressure at 100 °C

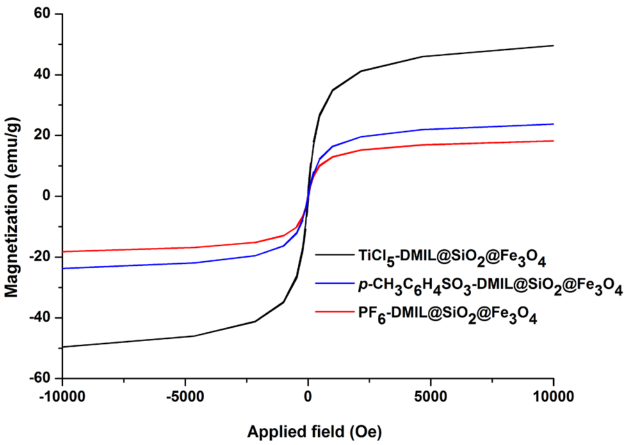

Fig. 8 Magnetization curves of PF_6-DMIL@SiO_2@Fe_3O_4, *p*-$CH_3C_6H_4SO_3$-DMIL@SiO_2@Fe_3O_4 and $TiCl_5$-DMIL@SiO_2@Fe_3O_4

through TG analysis (Fig. 10), the observed weight loss was associated with the loss of the organic components attached to the surface. In the TG curve, the observed organic materials weight loss of the IL showed a mass weight 34.8% on heating to 700 °C. The small weight loss before 110 °C is related to the desorption of adsorbed water and toluene, 9.1% weight loss occurred before 250 °C, indicating a considerably thermal stability up to 250 °C. There existed drastic weight loss between 250 and 500 °C is attributed to the breakdown of the organic moieties. From the curves depicted, it demonstrated that the supported IL is thermally stable below about 250 °C. The good thermal stability of $TiCl_5$-DMIL@SiO_2@Fe_3O_4 is beneficial to the recycling experiments, and the results showed that the product yield in each run with no notable decline in catalytic efficiency, suggesting that the catalyst could be recovered and recycled

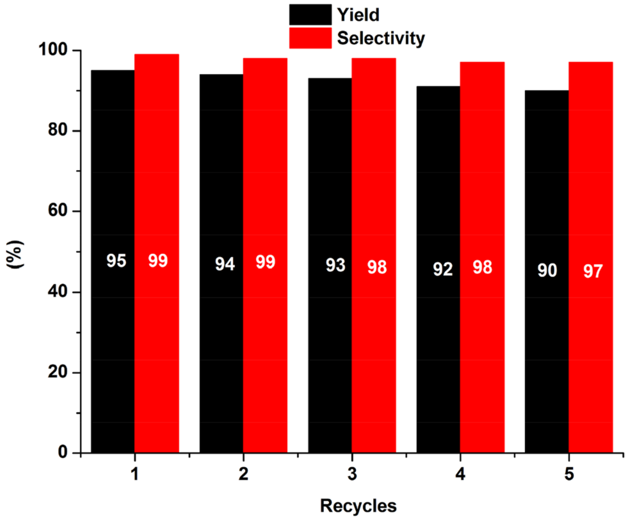

Fig. 9 Reusability of $TiCl_5$-DMIL@SiO_2@Fe_3O_4 in cycloaddition of propylene oxide and CO_2

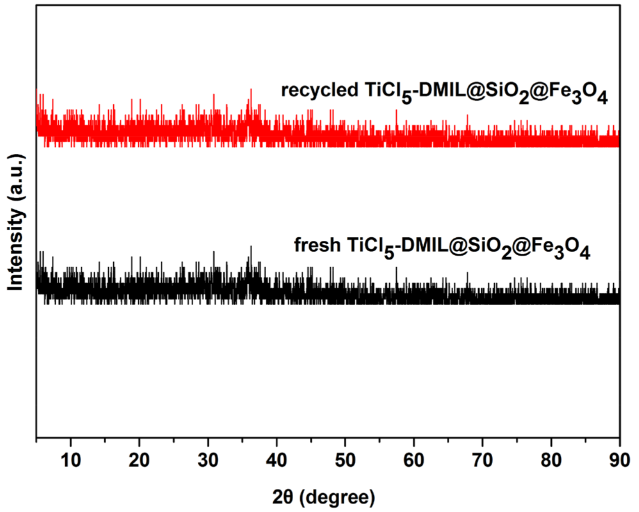

Fig. 11 XRD diffractogram of fresh and recycled $TiCl_5$-DMIL@SiO_2@Fe_3O_4

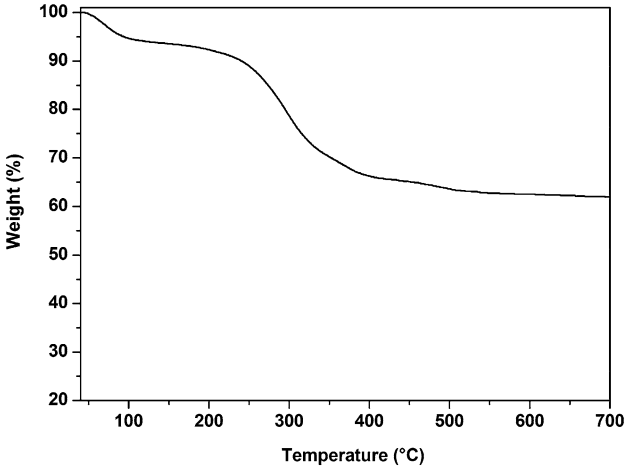

Fig. 10 TGA profile of $TiCl_5$-DMIL@SiO_2@Fe_3O_4

up to five runs with no significant loss of catalytic activities. The recovered catalyst after six runs had no obvious change in the morphology and size, referring to the SEM image in comparison with fresh catalyst (Fig. 2g). Furthermore, XRD diffractogram of the catalyst after five runs revealed that $TiCl_5$-DMIL@SiO_2@Fe_3O_4 preserved its original crystallinity during the reaction (Fig. 11).

In order to study the generality and scope of the catalyst $TiCl_5$-DMIL@SiO_2@Fe_3O_4, the catalytic activities of CO_2 with various epoxides were assessed and the results were shown in Table 2. A variety of epoxides were reacted with CO_2, which gave the desired cyclic carbonates in good to excellent yields (Table 2, entries 1–8). We found the catalyst showed high efficiency toward mono-substituted epoxides, and these cycloadditions proceeded smoothly and can be completed in 2 h (Table 2, entries 1, 4, 5, 7 and 8). However, di-substituted epoxides significantly decreased the reaction rate, and good yields were obtained after prolonged reaction time (Table 2, entries 3 and 6).

From these results, a possible reaction mechanism using the cycloaddition of propylene oxide with CO_2 as an example is proposed and depicted in Scheme 3 based on the previous literatures [12, 13, 34–37] and the observations in this reactions. At first, the substrate epoxide is activated by $TiCl_5$-DMIL@SiO_2@Fe_3O_4 to form the complex **1** by the coordination of one $TiCl_5$ anion with O atom of propylene oxide. Meanwhile, nucleophilic attack of the other $TiCl_5$ anion on the less sterically hindered carbon atom of propylene oxide the occurred to form the complex **2**, which reacts with CO_2 to produce complex **3**. Subsequent intramolecular substitution to afford the desired product.

4 Conclusion

In conclusion, series of silica coated magnetic nanoparticles supported ILs anion-DMIL@SiO_2@Fe_3O_4 were prepared and characterized. anion-DMIL@SiO_2@Fe_3O_4 was applied as a new heterogeneous solid catalyst in cycloaddition of CO_2 to epoxides successfully. Research shows that $TiCl_5$-DMIL@SiO_2@Fe_3O_4 is the most effective catalyst in the titled reaction. Various epoxides were reacted with CO_2 to give the corresponding cyclic carbonates in good to excellent yields with high selectivities under mild conditions. This methodology is endowed with

Table 2 Catalytic activity of the cycloaddition of various epoxides with CO_2

Entry	Epoxide	Product	Time (h)	Yield (%)[a]	Selectivity (%)[b]
1	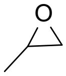	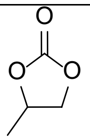	2	95	99
2		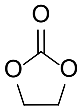	2	99	100
3	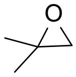	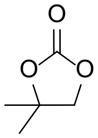	5	92	100
4	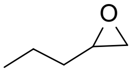	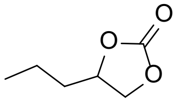	2	97	99
5	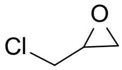	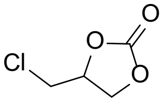	1	98	99
6	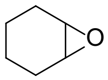	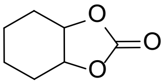	5	91	99
7	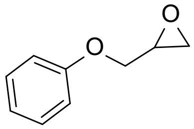	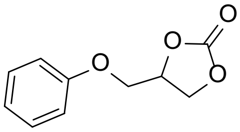	2	96	99
8	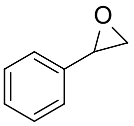	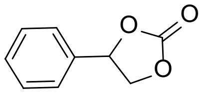	2	98	99

Reaction conditions: epoxide (0.1 mol), $TiCl_5$-DMIL@SiO_2@Fe_3O_4 (0.5 g), CO_2 (0.8 MPa), at 100 °C

[a] Isolated yield

[b] Isolated selectivity

some attractive features, such as short reaction times, high yields, simple experimental procedure, good generality, easy recoverability and recyclability of catalyst. Moreover, a possible mechanism is proposed. The above study would provide a green and efficient route towards the chemical carbon dioxide fixation.

Scheme 3 Possible mechanism for the cycloaddition

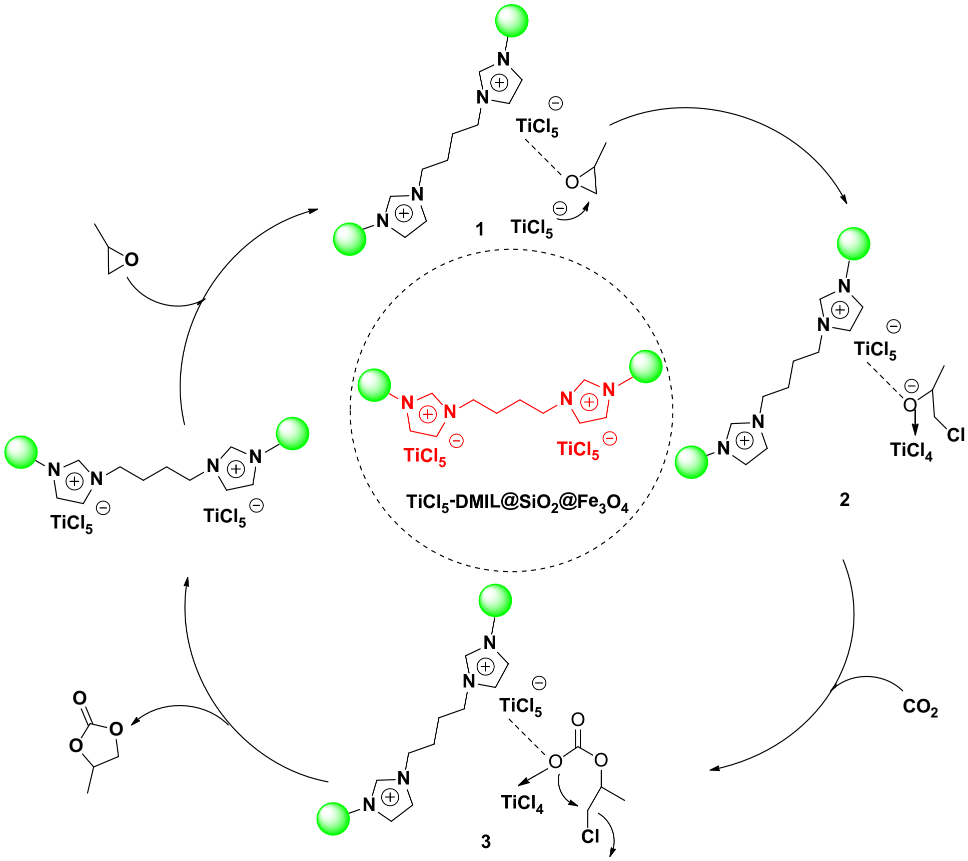

Acknowledgements The authors are grateful to the National Natural Science Foundation of China (No. 21506115) for financial support.

References

1. Goeppert A, Czaun M, Jones JP, Prakash GKS, Olah GA (2014) Chem Soc Rev 43:7995
2. Yang Z, Yu B, Zhang H, Zhao Y, Chen Y, Ma Z, Ji G, Gao X, Han B, Liu Z (2016) ACS Catal 6:1268
3. Lu XB, Darensbourg DJ (2012) Chem Soc Rev 41:1462
4. Monassier A, D'Elia V, Cokoja M, Dong H, Pelletier JDA, Basset JM, Kühn FE (2013) ChemCatChem 5:1321
5. Zhou X, Zhang Y, Yang X, Yao J, Wang G (2010) Chin J Catal 31:765
6. Siewniak A, Jasiak K, Baj S (2014) Appl Catal A 482:266
7. Meléndez J, North M, Villuendas P, Young C (2011) Dalton Trans 40:3885
8. Decortes A, Castilla AM, Kleij AW (2010) Angew Chem Int Ed 49:9822
9. Verma S, Kureshy RI, Roy T, Kumar M, Das A, Khan NH, Abdi SHR, Bajaj HC (2015) Catal Commun 61:78
10. Castro-Osma JA, Lamb KJ, North M (2016) ACS Catal 6:5012
11. Haak RM, Decortes A, Escudero-Adán EC, Belmonte MM, Martin E, Benet-Buchholz J, Kleij AW (2011) Inorg Chem 50:7934
12. Kozak JA, Wu J, Su X, Simeon F, Hatton TA, Jamison TF (2013) J Am Chem Soc 135:18497
13. Xie JN, Diao ZF, Qiao C, Ma R, He LN (2016) J CO2 Util 16:313
14. Babu R, Roshan R, Kathalikkattil AC, Kim DW, Park DW (2016) ACS Appl Mater Interfaces 8:33723
15. Morozan A, Jaouen F (2012) Energy Environ Sci 5:9269
16. Han YH, Zhou ZY, Tian CB, Du SW (2016) Green Chem 18:4086
17. Zalomaeva OV, Chibiryaev AM, Kovalenko KA, Kholdeeva OA, Balzhinimaev BS, Fedin VP (2013) J Catal 298:179
18. Yang DA, Cho HY, Kim J, Yang ST, Ahn WS (2012) Energy Environ Sci 5:6465
19. De D, Pal TK, Neogi S, Senthilkumar S, Das D, Gupta SS, Bharadwaj PK (2016) Chem Eur J 22:3387
20. Li PZ, Wang XJ, Liu J, Lim JS, Zou R, Zhao Y (2016) J Am Chem Soc 138:2142
21. Gao WY, Chen Y, Niu Y, Williams K, Cash L, Perez PJ, Wojtas L, Cai J, Chen YS, Ma S (2014) Angew Chem Int Ed 53:2615
22. Ema T, Fukuhara K, Sakai T, Ohbo M, Bai FQ, Hasegawa J (2015) Catal Sci Technol 5:2314
23. Sankar M, Ajithkumar TG, Sankar G, Manikandan P (2015) Catal Commun 59:201
24. Fiorani G, Guo W, Kleij AW (2015) Green Chem 17:1375
25. Büttner H, Steinbauer J, Werner T (2015) ChemSusChem 8:2655
26. Comerford JW, Ingram IDV, North M, Wu X (2015) Green Chem 17:1966
27. Cuesta-Aluja L, Castilla J, Masdeu-Bultó AM, Henriques CA, Calvete MJF, Pereira MM (2016) J Mol Catal A 423:489
28. Desens W, Kohrt C, Spannenberg A, Werner T (2016) Org Chem Front 3:156
29. Zou B, Hao L, Fan LY, Gao ZM, Chen SL, Li H, Hu CW (2015) J Catal 329:119
30. Cui G, Wang J, Zhang S (2016) Chem Soc Rev 45:4307

31. Steinrück HP, Wasserscheid P (2015) Catal Lett 145:380
32. Amarasekara AS (2016) Chem Rev 116:6133
33. Bobbink FD, Dyson PJ (2016) J Catal 343:52
34. Dai W, Yang W, Zhang Y, Wang D, Luo X, Tu X (2017) J CO2 Util 17:256
35. Liu M, Li X, Lin X, Liang L, Gao X, Sun J (2016) J Mol Catal A 412:20
36. Wang W, Li C, Yan L, Wang Y, Jiang M, Ding Y (2016) ACS Catal 6:6091
37. Dai WL, Chen L, Yin SF, Li WH, Zhang YY, Luo SL, Au CT (2010) Catal Lett 137:74
38. Pohako-Esko K, Bahlmann M, Schulz PS, Wasserscheid P (2016) Ind Eng Chem Res 55:7052
39. Sadeghzadeh SM (2016) J Mol Liq 223:267
40. Fehér C, Kriván E, Hancsók J, Skoda-Földes R (2012) Green Chem 14:403
41. Xin B, Hao J (2014) Chem Soc Rev 43:7171
42. Sefat MN, Saberi D, Niknam K (2011) Catal Lett 141:1713
43. Yang J, Zhou L, Guo X, Li L, Zhang P, Hong R, Qiu T (2015) Chem Eng J 280:147
44. Bagheri M, Masteri-Farahani M, Ghorbani M (2013) J Magn Magn Mater 327:58
45. Chen Y, Zhang F, Fang Y, Zhu X, Zhen W, Wang R, Ma J (2013) Catal Commun 38:54
46. Rostamizadeh S, Nojavan M, Aryan R, Azad M (2014) Catal Lett 144:1772
47. Biagini P, Bonoldi L, Marchetti F, Pampaloni G (2010) Inorg Chim Acta 363:3637
48. Weiß T, Natarajan K, Lang H, Holze R (2002) J Electroanal Chem 533:127
49. Grabow K, Bentrup U (2014) ACS Catal 4:2153